Received: 25 July 2023 | Accepted: 16 September 2024

DOI: 10.1002/vzj2.20384

Vadose Zone Journal

ORIGINAL ARTICLE

Estimating soil moisture from environmental gamma radiation monitoring data

Sonia Akter | **Johan Alexander Huisman** | **Heye Reemt Bogena**

Agrosphere Institute (IBG-3), Forschungszentrum Jülich GmbH, Jülich, Germany

Correspondence
Sonia Akter, Agrosphere Institute (IBG-3), Forschungszentrum Jülich GmbH, 52428 Jülich, Germany.
Email: s.akter@fz-juelich.de

Assigned to Associate Editor Narendra Das.

Funding information
Deutsche Forschungsgemeinschaft, Grant/Award Number: SFB 1502/1–2022 - Projektnummer: 450058266

Abstract

Soil moisture (SM) information is invaluable for a wide range of applications, including weather forecasting, hydrological and land surface modeling, and agricultural production. However, there is still a lack of sensing information that adequately represents root-zone SM for longer periods and larger spatial scales. One option for root-zone SM observation is terrestrial gamma radiation (TGR), as it is inversely related to SM. Hence, the near real-time data of more than 5000 environmental gamma radiation (EGR) monitoring stations archived by the EUropean Radiological Data Exchange Platform (EURDEP) is a potential source to develop a root-zone SM product for Europe without extra investments in SM sensors. This study aims to investigate to what extent the EURDEP data can be used for SM estimation. For this, two EGR monitoring stations were equipped with in situ SM sensors to measure reference SM. The terrestrial component of EGR was extracted after eliminating the contributions of rain washout and secondary cosmic radiation, and used to obtain a functional relationship with SM. We predicted the weekly volumetric SM with a root mean square error of 7%–9% from TGR measurements. Nevertheless, we believe that this technique, due to its greater penetration depth and long data legacy, can provide useful data complementary to satellite-based remote sensing techniques to estimate root-zone SM at the continental scale.

Plain Language Summary

Information on the temporal dynamics of SM across a large area is vital for many sectors. An extensive network for monitoring EGR detectors that has been operated across Europe after the Chernobyl nuclear accident is a potential source for deriving continental-scale SM information without additional costs. We investigated how accurately SM can be estimated from the data of two of such detectors. The results showed that weekly SM estimates with an accuracy of 0.07–0.09 cm^3 cm^{-3} are

Abbreviations: AR, artificial radiation; EGR, environmental gamma radiation; EURDEP, EUropean Radiological Data Exchange Platform; SCR, secondary cosmic radiation; SM, soil moisture; TGR, terrestrial gamma radiation; TS1, test site 1; TS2, test site 2.

feasible after adequate data processing accounting for other factors affecting EGR. We also discussed possible sources that affected the accuracy of the SM estimates and provided directions for further research. Despite the current limitations, EGR data show potential for estimating SM across Europe.

1 | INTRODUCTION

Soil moisture (SM) information is invaluable for a wide range of sectors concerned with weather and climate (Mishra et al., 2017; Stahlmann-Brown & Walsh, 2022), runoff potential and flood control (Ghajarnia et al., 2020; Ran et al., 2022; Singh et al., 2021), soil erosion and slope failure (Moragoda et al., 2022), geotechnical engineering (N. Lu, 2019), and water quality (Pignotti et al., 2023). A wide range of methods are available to measure spatial and temporal SM dynamics, such as point measurements by gravimetric sampling or using electromagnetic sensors, sensor networks, geophysical measurements, and airborne and space-borne remote sensing (Vereecken et al., 2022). All these methods have their own strengths and limitations. For instance, due to the high spatial variability of SM, it requires many point measurements to accurately represent SM at larger scales. Although wireless sensor networks can provide SM measurements with high temporal resolution (Bogena, Weuthen, et al., 2022), the spatial extent of such networks is typically still relatively small. Geophysical methods like ground penetrating radar and electromagnetic induction are promising methods to obtain qualitative SM information with a high spatial resolution up to the catchment scale (Binley et al., 2015). However, quantitative SM predictions with these methods are often not satisfactory due to the uncertainties in the petrophysical models linking geophysical properties to SM (Terry et al., 2023). Moreover, geophysical methods are labor-intensive and not suitable for long-term monitoring. Airborne remote sensing surveys can cover areas up to 100 km^2, but the costs are generally considered to be excessive for SM measurements. Space-borne measurements have the advantage of global coverage, but they are often associated with a low measurement depth and low accuracy, especially in case of dense vegetation (Bogena et al., 2015). Therefore, there is a need for new sources of information for monitoring the variability of root-zone SM, particularly at regional to continental scales.

One potential source of such information is terrestrial gamma radiation (TGR), which is the radiation originating from the decay of radionuclides that are naturally present in the soil, for example, ^{40}K, ^{232}Th, and ^{238}U. In the 1970s–1980s, a few studies reported that airborne surveys with low-flying airplanes using spectrally resolved TGR sensors can be used to determine SM (Carroll, 1981) and snow water equivalent (Peck et al., 1971). The measurement principle is based on the increasing attenuation of TGR with increasing SM. However, it is difficult to determine SM quantitively from airborne TGR surveys because the spatial distribution of radionuclides that determine the background radiation is not known (Bogena et al., 2015). Therefore, TGR measurements from permanently installed ground-based stations can be more promising than the TGR measurements from airborne surveys in terms of measurement accuracy and operational cost (Bogena et al., 2015). Although some earlier studies attempted to quantitively relate SM with ground-based spectroscopic TGR measurements (e.g., Loijens, 1980; Yoshioka, 1989), recent technical advancements are opening up new prospects in the development of noninvasive gamma-ray proximal sensors to monitor SM dynamics. For example, Baldoncini et al. (2018) established that proximal gamma-ray spectroscopy to measure the temporal changes in TGR is a promising approach to determine SM with an average uncertainty of <1%. Strati et al. (2018) also reported the potential of gamma-ray spectroscopy for the successful estimation of daily SM dynamics over a 7-month period. In their study, they estimated SM for an area with a radius of 25 m and a depth of 30 cm using a sensor at a height of 2.25 m. Similarly, van der Veeke et al. (2020) developed a new type of sensor (gamma SM Sensor [gSMS]) that uses measurements of TGR to estimate SM. Gianessi, Polo, Stevanato, Lunardon, and Baroni (2022) reported that gamma-ray spectroscopy can capture the SM dynamics as accurately as the more established cosmic-ray neutron sensing technique (Andreasen et al., 2020; Bogena, Schrön, et al., 2022; Zreda et al., 2012) for a large, cropped field in Italy. In all these studies, TGR measurements were made with scintillation-based spectroscopic sensors that determine radiation in a specific energy window (i.e., ^{40}K photopeak at 1.46 MeV) for which a clear SM signal can be expected.

After the nuclear reactor accident in Chernobyl in 1986, most countries of the European Union (EU) established in situ monitoring networks measuring environmental gamma radiation (the total amount of outdoor gamma radiation emitted from all ambient sources including soil) (EGR) to provide early warning. These EGR measurements are archived and published in near real-time by the EUropean Radiological Data Exchange Platform (EURDEP) (REMon, 2024a). As a result, measurements of more than 5000 monitoring

stations are available (Figure 1). Detailed information about the EURDEP status and data availability can be found in Sangiorgi et al. (2020). The possibility to determine SM from this monitoring network is attractive because it would allow to obtain Europe-wide information on SM without extra investments (Stöhlker et al., 2012). However, the EURDEP network mostly provides integrated EGR measurements from gas-filled gamma-ray sensors, that is, Geiger-Müller and proportional counter tubes, which count the number of gamma photons entering the detector over a broad energy spectrum (i.e., 0–3 MeV) without distinguishing between photon energies (Dombrowski et al., 2017). This type of sensor is optimized for radiation protection tasks, for example, for measuring the local radiation dose rate in long-term continuous operation. Moreover, these sensors are simpler and less expensive to maintain than the scintillation-based spectroscopic sensors (Dombrowski et al., 2017). So far, models for estimating SM from TGR have only been developed for the high-energy range, for example, for the energy of photons from K-40 decay in soils (e.g., Baldoncini et al., 2018; Carroll, 1981; Loijens, 1980). Studies that test whether such models can also be applied to EGR measurements from gas-filled gamma-ray sensors that measure in a broad energy range are still missing. Moreover, the physics behind EGR measurements with regard to SM prediction is not yet clearly understood. For example, there is a lack of understanding on the energy dependency of EGR sensors in heterogeneous ambient conditions as well as the influence of meteorological and other confounding factors on the EGR signal and how this affects SM prediction accuracy. Although Stöhlker et al. (2012) already presented the correlation between EGR and SM for a period of 2 months, neither did they develop a functional relationship between SM and EGR nor did they address meteorological and other confounding factors for a longer period. Thus, there is a considerable scope for an improved evaluation of the potential of EURDEP data for SM estimation.

The aim of this study is to better understand the measurement data from gas-filled gamma-ray sensors typically used in EURDEP for measuring the local radiation dose rate and to investigate how accurately SM can be estimated from these EGR measurements over a broad energy range. The remainder of this paper is organized as follows: First, the fundamentals of gamma-ray attenuation and detection are presented. Next, a calibration method to obtain SM from TGR is derived based on established physics. In addition, the meteorological influences on EGR are evaluated to improve the accuracy of SM estimation. Finally, multi-year TGR measurements are used to estimate weekly SM and compared with in situ SM measurements to evaluate the accuracy of the SM estimates. This study ends with a discussion of possible sources of SM prediction uncertainty when using EGR measurements over a broad energy range.

Core Ideas

- An extensive early warning monitoring network for environmental gamma radiation (EGR) is maintained in Europe.
- Since soil moisture influences EGR, this database could be used to derive continental soil moisture products.
- To test this, two monitoring stations in Germany were selected and equipped with reference soil moisture sensors.
- From the terrestrial component of EGR, soil moisture was determined with an error of 7–9 vol.%.

2 | THEORY

2.1 | Sources of environmental gamma radiation

With a gas-filled sensor, the EGR is measured according to the ambient dose equivalent, H*(10) in nSv h^{-1}, which is used to quantify the risk of radiation exposure to human health. For the exact definition of the ambient equivalent dose, the reader is referred to Vana et al. (2003). In this study, we use "EGR" when we refer to the measurements with gas-filled sensors and replace the symbol "H*(10)" by "R" for simplicity. According to Neumaier and Dombrowski (2014), the measured EGR (R) consists of four components:

$$R = R_{\mathrm{TGR}} r_{\mathrm{TGR}} + R_{\mathrm{SCR}} r_{\mathrm{SCR}} + R_{\mathrm{AR}} r_{\mathrm{AR}} + R_B \qquad (1)$$

where R_{TGR}, R_{SCR}, and R_{AR} represent terrestrial gamma radiation (TGR), secondary cosmic radiation (SCR), and radiation due to artificial sources (AR), respectively. The parameters r_{TGR}, r_{SCR}, and r_{AR} are the response factors for TGR, SCR, and AR, respectively. The response factors of both TGR and AR depend on the energy spectra of the radiation (Kessler et al., 2018). Typical values for the response factors range from 0.7 to 1.3 (Thermo, 2015). The response factor for R_{SCR} additionally depends on the orientation of the sensor (Dombrowski & Wissmann, 2008). The R_B is the intrinsic background or self-effect of the instrument, which also depends on source energy and needs to be determined experimentally (Bossew et al., 2017; Neumaier & Dombrowski, 2014). The R_B may be affected by automatic corrections made by the measurement system. It can be positive or negative by up to 10 nSv h^{-1} for a proportional counter-tube sensor and by 7–41 nSv h^{-1} for a Geiger–Müller sensor (Szegvary et al., 2007). Sensors of the same type may show a considerable variability of the R_B, and differences between individual probes can be as high as 5%–10% (Szegvary et al., 2007).

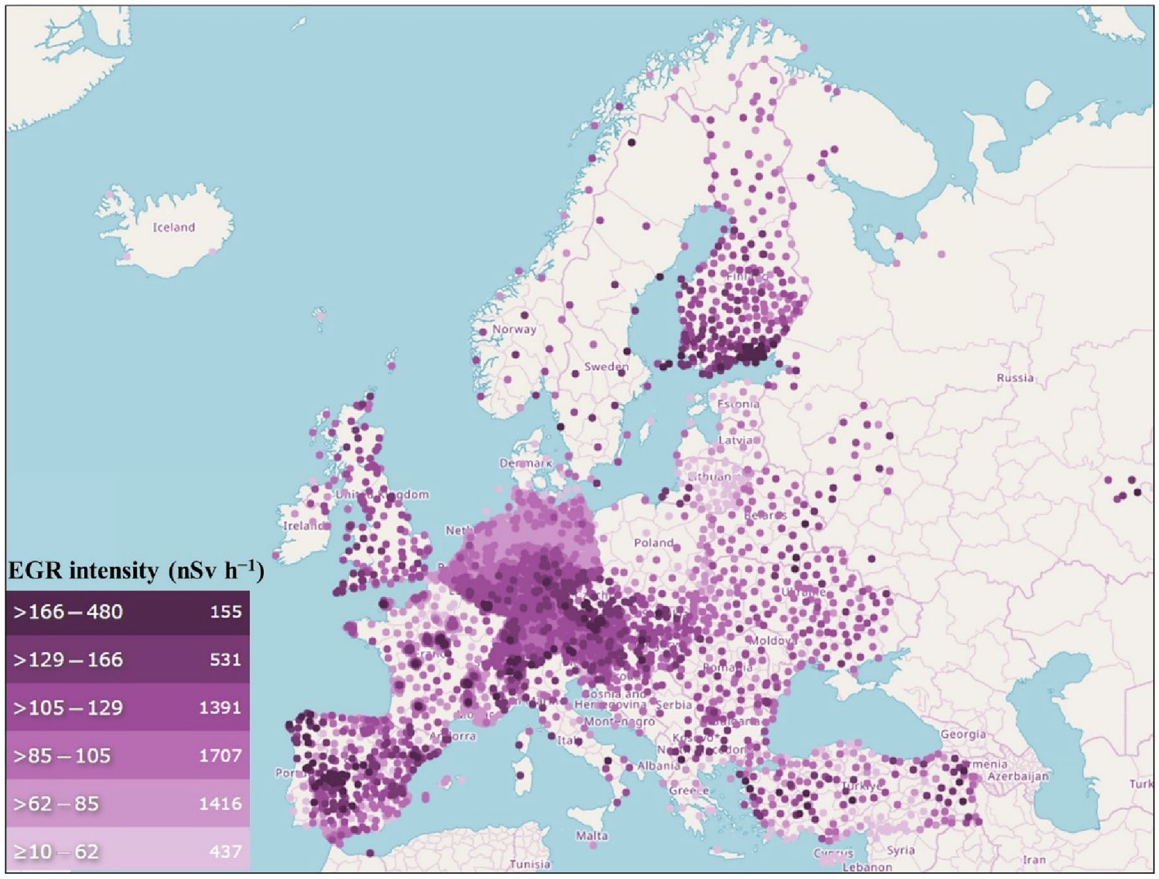

FIGURE 1 The mean environmental gamma radiation (EGR) observed by the EUropean Radiological Data Exchange Platform (EURDEP) network between July 6 and 13, 2023 (REMon, 2023). The right-hand numbers in the legend indicate the number of stations in the respective intervals.

It is important to note that temperature variability is also responsible for the uncertainty in R_B measurements (Stöhlker et al., 2019). However, temperature-dependent changes in R_B are typically well below 5 nSv h^{-1} for a change of temperature from −20 to 55°C (Stöhlker et al., 2019). During normal times (without any nuclear accident or emergency), the measurements of EGR sensors reflect the natural radiation background, where TGR and SCR are the main contributors to EGR. Hence, we restrict the discussion to these two components in the following.

2.1.1 | Terrestrial gamma radiation

TGR can originate from both anthropogenic and natural sources. The main source of anthropogenic TGR is the ^{137}Cs radionuclide deposited on the ground by fallout from nuclear bomb testing and accidents in nuclear plants, for example, Chernobyl (Szegvary et al., 2007). The contribution of these anthropogenic sources to EGR is generally small (Bossew et al., 2017). Hence, the high-energy radionuclides such as ^{40}K, ^{232}Th, and ^{238}U as well as the associated decay products are considered as the main contributions to TGR (Bossew et al., 2017). These isotopes are abundant in the soil and have half-lives in the same order of magnitude as the age of the earth. Depending on the geological setting, TGR contributes ∼20–200 nSv h^{-1} to the EGR measured at ground level (UNSCEAR, 2000).

Radon is a radioactive noble gas, which has 39 known isotopes ranging from ^{193}Rn to ^{231}Rn. The most stable isotope ^{222}Rn with a half-life of 3.823 days is present in the decay chain of ^{238}U, which occurs naturally in different levels in all rocks and soils. Although ^{222}Rn primarily originates in the soil, it does not bind to soil particles. As a result, it can move with the air through pores and fractures and can escape from the soil to the atmosphere. Hence, radon is ubiquitous in the air at ground level and may have a significant contribution to the temporal dynamics of TGR. In dry periods, diurnal fluctuations in EGR have been observed, which were attributed to temperature inversion layers in the atmosphere that retained radon and radon progenies during the night causing a nighttime increase in EGR (Greenfield et al., 2002). After sunrise, warm near-surface air destroyed this temperature inversion layer causing a decrease in EGR (Greenfield et al., 2002).

It is well known that precipitation washes radon progenies (mostly ^{214} Pb and ^{214}Bi) out of the atmosphere, leading to abrupt increases in EGR observations (up to 300 nSv h^{-1}) associated with precipitation events (Bossew et al., 2017; Dombrowski & Wissmann, 2008). The magnitude of this effect differs between precipitation events. In general, longer rain events do not lead to a higher increase in EGR compared to shorter rain events because the atmosphere is cleaned quickly due to the rain wash-out and the transport of radon to the higher atmosphere is relatively slow (Bossew et al., 2017). After the cessation of rainfall, the EGR due to this wash-out starts to decrease exponentially as a result of the decay of these short-lived (~20 min) radon progenies. About 3 h after a rainfall event, the increase in EGR due to atmospheric radon progenies typically has ceased (Minty, 1997). The presence of a snow cover also affects EGR because it shields TGR emitted from the soil (Bleher et al., 2014).

2.1.2 | Secondary cosmic radiation

Secondary cosmic rays are the products of the collision of primary cosmic rays (coming from outer space) with the atoms of the Earth's atmosphere (Morison, 2008). Muons are the major component of cosmic radiation at ground level in addition to electrons, positrons, neutrons, and gamma rays. In Central Europe, the SCR is approximately 40 nSv h^{-1} at ground level to which muons contribute with 50%, neutrons with 20%, and electrons, positrons, and photons with 30% (Wissmann & Sáez-Vergara, 2006; Wissmann et al., 2005). The SCR depends on latitude and altitude. The SCR is lower in low latitudes compared to high latitude areas (Bobik et al., 2012). With increasing altitude, the proportion of SCR in EGR increases (Wissmann et al., 2007). Other parameters such as air pressure, solar activity, and temperature also influence the fluctuations of SCR (Bogena, Schrön, et al., 2022). The relationship between SCR (for both charged and neutral components) and atmospheric pressure can be described as follows (Dombrowski & Wissmann, 2008):

$$\Delta R_{\mathrm{SCR},\,\mu} = -C_{\mu}\Delta p \tag{2}$$

$$\Delta R_{\mathrm{SCR},\,n} = -C_{n}\Delta p \tag{3}$$

where $\Delta R_{\mathrm{SCR},\mu}$ is the difference in SCR due to the charged components, C_{μ} is a factor for the charged components with a value of 0.051 nSv h^{-1} hPa^{-1}, $\Delta R_{\mathrm{SCR},n}$ is the difference in SCR due to neutral components (e.g., neutrons), C_n is a factor for neutrons with a value of 0.076 nSv h^{-1} hPa^{-1}, and Δp is the air pressure difference relative to the standard air pressure.

The components of SCR, especially neutrons and muons, are also known to be inversely related to solar activity (Dombrowski & Wissmann, 2008). The variations in SCR due to the changes in solar activity might range from 10% to 20% and is subject to an 11-year cycle (Dombrowski & Wissmann, 2008). The fluctuations in neutron flux due to solar activity can be described by:

$$\Delta R_{\mathrm{SCR},\,n} = 1 + \Delta N_{m} \tag{4}$$

where $\Delta R_{\mathrm{SCR},n}$ is the difference in SCR due to neutrons and ΔN_m is the relative deviation of the neutron count from the average neutron count rate. The muon and neutron fluxes at the ground level are highly correlated (Stevanato et al., 2022), and, therefore, the fluctuations in muon flux due to solar activity can be estimated by:

$$\Delta R_{\mathrm{SCR},\,\mu} = 1 + C_{nm}\Delta N_{m} \tag{5}$$

where $\Delta R_{\mathrm{SCR},\mu}$ is the difference in SCR due to muons, and C_{nm} is a factor with a value of 0.52 ± 0.05 as reported by Wissmann (2006). Finally, the seasonal variation of atmospheric temperature also influences the muon flux on the ground. However, the influence of this factor is small and only leads to a deviation of SCR by $\pm$ 1.5 nSv h^{-1} (Dombrowski & Wissmann, 2008). Therefore, this factor was neglected here. It should be noted that the described corrections for the SCR component of EGR measurements are similar to the corrections for cosmic-ray neutron measurements (Zreda et al., 2012), except that the latter technique requires an additional correction for atmospheric humidity because of its sensitivity to the total amount of hydrogen within the measurement footprint (Rosolem et al., 2013).

2.2 | Gamma ray attenuation

Gamma-rays are attenuated by interactions with matter. There are three types of interactions: the photoelectric effect, Compton scattering, and pair production. The relative importance of these interactions for gamma-ray attenuation depends on the energy of the gamma rays (IAEA, 2003). Compton scattering is the dominant type of interaction for the energy range associated with TGR (Baldoncini et al., 2018; Minty, 1997). The incident gamma-ray photons lose part of their energies to the electrons of the interacting medium during each scattering event, and eventually the resulting low-energy photons are absorbed completely by the electrons through the photoelectric effect (Minty, 1997). Thus, the attenuation of TGR is proportional to the electron density of the material. The simplest approach for modeling gamma-ray attenuation is based on mono-energetic radiation through a homogenous material that follows the classical Beer-Lambert law of absorption:

$$I = I_0 e^{-(\mu x)} \tag{6}$$

where I is the gamma radiation after passing through a material of thickness x, I_0 is the initial gamma radiation, and μ is the linear attenuation coefficient. For different materials, the mass attenuation coefficient ($\mu_m = \mu/\rho$) is an intrinsic property that strongly depends on the energy level of gamma-rays (Grasty, 1976).

In porous media such as soil, gamma-rays are attenuated by the solid, water, and air phase of soil. Therefore, Equation (6) can be extended by considering the fractions (θ) and density (ρ) of the solid, water, and air phase (Beamish, 2013):

$$I = I_0 e^{-(\mu_{m,s}\theta_s\rho_s x + \mu_{m,w}\theta_w\rho_w x + \mu_{m,a}\theta_a\rho_a x)} \quad (7)$$

where the subscripts s, w, and a refer to the solid, water, and air phase, respectively. Values for the three mass attenuation coefficients as a function of photon energy can be found in the NIST database (NIST, 2024) for the energy range between 0.01 and 3 MeV. As the density of air is three orders of magnitude lower than the density of the water and the solid phase, the attenuation by the air phase in the soil can be neglected. The linear attenuation coefficient for the solid phase depends only on the mineral types in the soil, in particular the average density and atomic number of the elements contained in the minerals. Therefore, it is reasonable to assume that the attenuation by the solid fraction (θ_s) is constant, and that changes in gamma-ray attenuation mainly depend on the water content of the soil. Water is ~1.11 times more effective in attenuating TGR than a typical solid material because water has 1.11 times as many electrons per weight compared to solid material (Grasty, 1976). Hence, the ratio of mass attenuation coefficients for water and solid phases, $\frac{\mu_{m,w}}{\mu_{m,s}}$, is 1.11. It is interesting to note that this value of 1.11 is valid for radionuclides with an energy range from 0.4 to 1.46 MeV, and that the ratio $\frac{\mu_{m,w}}{\mu_{m,s}}$ is expected to be lower than 1.11 for low-energy nuclides (NIST, 2024). The value of $\frac{\mu_{m,w}}{\mu_{m,s}}$ as a function of energy is provided in Figure S1.

2.3 | Gamma radiation measurement volume

The measurement volume of the EGR sensor is the volume from where the gamma radiation signal originates. It characterizes the scale and spatial resolution of the SM estimates obtained from EGR measurements. If the sensor is placed at 1 m height, 95% of the detected signal originates from within a radius of 15 m around the sensor for the decay of ^{40}K at 1.46 MeV (Baldoncini et al., 2018). An increase in sensor height will result in a larger horizontal footprint (van der Veeke et al., 2020). The horizontal footprint of the EGR sensor is not strongly dependent on SM (Beamish, 2013). Regarding the vertical footprint of the EGR sensor, 95% of the detected gamma radiation signal originates from the top 30 cm of soil in case of a bulk density of 1.2 g cm^{-3} at 1.46 MeV (Baldoncini et al., 2018). The sensing depth decreases with increasing bulk density of the soil. More information on the horizontal and vertical footprint of EGR sensors can be found in Baldoncini et al. (2018).

2.4 | Relationship between gamma radiation and soil moisture

For a sensor with cross-sectional area, A, photopeak efficiency, ε, installed at a height, h, the number of gamma-ray photons recorded per second, N, originating from an infinite homogeneous soil volume source is given by Grasty (1976):

$$N = \frac{nA\varepsilon}{2\mu_g} E_2\left(\mu_a h\right) \quad (8)$$

where n is the number of emitted photons per unit volume of soil per second, μ_a is the linear attenuation coefficient for air, μ_g is the linear attenuation coefficient for the ground, and E_2 indicates a function known as the exponential integral of the second kind given by:

$$E_2\left(\mu_a h\right) = \int_1^\infty \frac{e^{-\mu_a h x}}{x^2} dx \quad (9)$$

where x is the thickness of the air layer between the soil and the sensor. The relative change in gamma-ray photon count rate due to the presence of SM can be derived from Equation (8) as:

$$\frac{N}{N_{\text{dry}}} = \frac{\frac{nA\varepsilon}{2\mu_g} E_2\left(\mu_a h\right)}{\frac{nA\varepsilon}{2\mu_{g,\text{dry}}} E_2\left(\mu_a h\right)} = \frac{\mu_{g,\text{ dry}}}{\mu_g} \quad (10)$$

where N_{dry} is the gamma-ray photon count rate and $\mu_{g,\text{dry}}$ is the linear attenuation coefficient for the ground in a dry state without water.

To investigate the influence of SM on gamma-ray attenuation in soil, the differences in attenuation between wet and dry soil can be quantified considering the ratio of mass attenuation coefficients for water and solid phases ($\frac{\mu_{m,w}}{\mu_{m,s}}$) (Figure S1). For high-energy nuclides, the relationship between μ_g and $\mu_{g,\text{dry}}$ is given by Løvborg (1984):

$$\mu_g = \mu_{g,\text{dry}}\left[1 + 1.11\, w\right] \quad (11)$$

where w is the gravimetric water content (g g^{-1}). By combining Equations (10) and (11), it can be shown that:

$$\frac{N}{N_{\text{dry}}} = \frac{1}{1 + 1.11\ w} \tag{12}$$

Considering volumetric SM, Equation (12) can be rewritten as:

$$\frac{N}{N_{\text{dry}}} = \frac{1}{1 + 1.11\ \frac{\theta \rho_w}{\rho_b}} \tag{13}$$

where θ is the SM in vol.%, ρ_w is the density of water, and ρ_b is the dry bulk density of soil.

The normalized TGR as a function of the volumetric water content is shown in Figure 2 based on Equation (13). The relationship between these two variables is expected to be approximately linear and only dependent on soil bulk density. The EGR sensors used for the current study record the total EGR in a broad energy band ranging from 0 to 3 MeV. Since the effective energy of the TGR is not known, we introduce α as the effective ratio of the mass attenuation coefficients for water and solid phases for TGR and modified Equation (13) accordingly:

$$\frac{R_{\text{TGR}}}{R_{\text{TGR,dry}}} = \frac{1}{1 + \alpha\ \frac{\theta \rho_w}{\rho_b}} \tag{14}$$

If the dry bulk density of soil is known, the two remaining parameters $R_{\text{TGR,dry}}$ and α in Equation (14) can be calibrated using TGR and reference SM measurements. After calibration, SM can be predicted from TGR with:

$$\theta = \frac{\rho_b \left(R_{\text{TGR,dry}} - R_{\text{TGR}}\right)}{\alpha\ R_{\text{TGR}}} \tag{15}$$

3 | MATERIALS AND METHODS

3.1 | Experimental site

Two EGR monitoring stations of the Forschungszentrum Jülich GmbH (FZJ), Germany (N50°91′, E6°40′) were considered for the current study. The land use in the surroundings of both monitoring stations is heterogeneous (a mix of grass, shrubs, and deciduous trees), which is also the case for many EURDEP stations (Dombrowski et al., 2017). The monitoring stations are named test site 1 (TS1) and test site 2 (TS2) for the current study (Figure 3). Overview photos of both TS1 and TS2 are provided in Figures S2 and S3. Both sites show moderate soil radioactivity and the values of activity concentrations for different soil radionuclides can be found in REMon (2024b). A 4-year time series (January 1, 2014, to January 1, 2018) of EGR measurements was considered for this study.

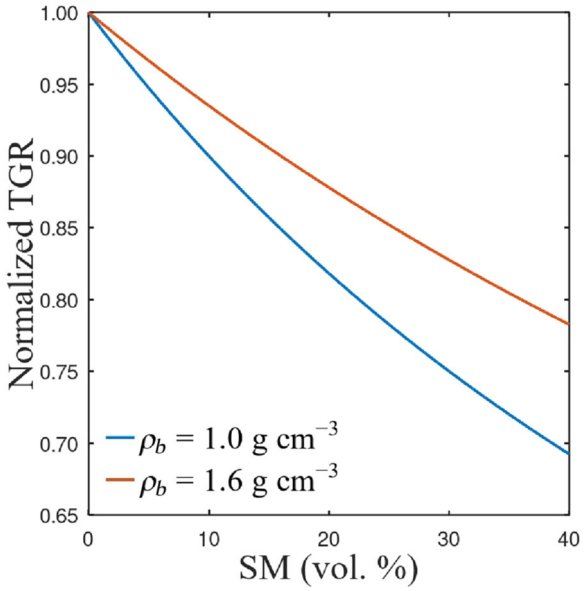

FIGURE 2 Theoretically derived normalized terrestrial gamma radiation (TGR) as a function of soil moisture (SM) for a high and low soil bulk density (ρ_b). This relationship is valid for an energy range of 0.4–1.46 MeV.

3.2 | Environmental gamma radiation monitoring sensors

The EGR was measured by proportional counters of the type FHZ 621 G-L (Thermo Fisher Scientific Inc.). The sensors were installed to monitor the EGR as an early warning for nuclear exposure. The proportional counter consists of a gas-filled cylindrical tube (length 340 mm, external diameter 65 mm) that contains a mixture of argon and carbon dioxide. The sensors are mounted on a pole 1 m above the ground with a PE protection cover (Figure 3) and monitor EGR with 10-min integration time. For this integration time, the measurement error is ±6% in the range from 50 nSv h^{-1} to 0.1 Sv h^{-1} (Thermo, 2015). The approximate energy range of proportional counters ranges from 26 keV to 3 MeV (Thermo, 2015). Proportional counters may offer a lower energy dependence of the response (Dombrowski et al., 2017), and the energy dependency for the counters used in this study was ±30% in the range from 30 keV to 1.3 MeV (Thermo, 2015). Proportional counters can be used in different modes with a possibility to obtain energy dependence compensation (Thompson et al., 1999). However, sensors used for the current study measured EGR in counting mode, which is the simplest mode that detects radiation without providing information on its energy. This is similar to the

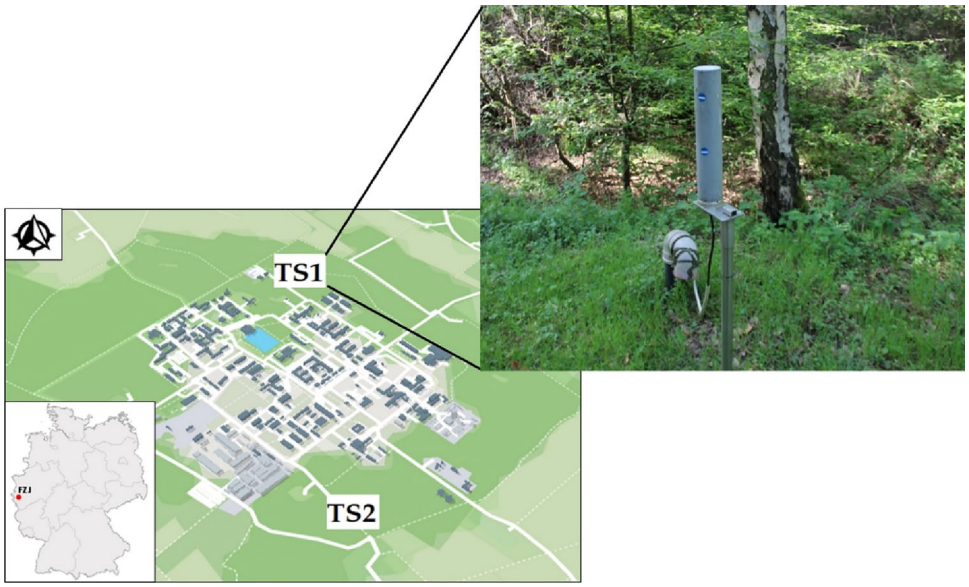

FIGURE 3 Locations of the environmental gamma radiation (EGR) monitoring stations on the premises of the Forschungszentrum Jülich (TS1, test site 1; TS2, test site 2).

conventional EURDEP gamma-ray sensors. However, the various sensor types from different companies used in the EURDEP network differ in terms of sensitivity, self-effect, energy dependency, and linearity of the response, as well as the response to SCR. Detailed information on the accuracy and measurement characteristics of gamma-ray sensors used in the EURDEP network can be found in Stöhlker et al. (2009). Nevertheless, it is important to stress here that the EGR sensor type investigated in this study is representative for the general behavior of sensors in the EURDEP network.

3.3 | Extracting the terrestrial component of environmental gamma radiation

In a first step, transient increases in the EGR measurements during and after precipitation due to wash-out of radon progenies were removed using data filtering. For this, periods with precipitation and up to 3 h after precipitation were identified and excluded from further analysis. The required precipitation data for this filtering were measured by a climate station located inside the campus of FZJ with a temporal resolution of 10 min.

In a second step, the long-term constant contribution of SCR was removed while also considering its short-term variability due to atmospheric pressure and solar activity. We assumed that the long-term contribution of SCR was the same for both test sites, which is reasonable given the proximity of the sensors. Atmospheric pressure measurements were not available for the same climate station where precipitation was recorded. Hence, these data were obtained from a nearby climate station at the lysimeter facility also located on the FZJ campus. To account for the short-term SCR variability, we used incoming neutron flux data from the neutron monitor database (NMDB; https://www.nmdb.eu/nest/). The closest station for the study area is Jungfraujoch (JUNG), located in Switzerland. Using Equations (2)–(5), the variability in SCR was described as:

$$R\prime_{\mathrm{SCR}} = \left(R_{\mu,\,\mathrm{mean}} - 0.051\left(P - P_{\mathrm{ref}}\right)\left(1 + 0.52 \times \Delta N_m\right)\right) + \left(R_{n,\,\mathrm{mean}} - 0.076\left(P - P_{\mathrm{ref}}\right)\left(1 + \Delta N_m\right)\right) \quad (16)$$

where R'_{SCR} is the corrected SCR, $R_{\mu,\mathrm{mean}} = 32.7$ nSv h^{-1} is the average muon flux at sea level reported by Dombrowski and Wissmann (2008), $R_{n,\mathrm{mean}} = 8$ nSv h^{-1} is the average neutron flux at sea level reported by Wissmann et al. (2005), $P_{\mathrm{ref}} = 1013.25$ is the standard atmosphere pressure at sea level, and P is the actual atmospheric pressure at the test site. After estimating R'_{SCR}, the TGR can be derived from Equation (1) using:

$$R_{\mathrm{TGR}} = r_{\mathrm{TGR}}^{-1}\left(R - R_B - r_{\mathrm{AR}}R_{\mathrm{AR}} - r_{\mathrm{SCR}}R\prime_{\mathrm{SCR}}\right) \quad (17)$$

Unfortunately, the response factors and the inherent sensor background/self-effect (R_B) were not known for the sensors used for this study. Therefore, the response factors were assumed to be 1 and the measurements were not corrected for a self-effect. Furthermore, we did not consider the contribution of AR. With these simplifications, Equation (17) reduces to:

$$R_{\mathrm{TGR}} = R - R\prime_{\mathrm{SCR}} \quad (18)$$

3.4 | Reference soil moisture measurements with SoilNet

At both sites, a SoilNet SM station was installed within the measurement footprint of the EGR monitoring station to measure reference SM. SoilNet is a wireless sensor network that enables real-time SM monitoring with a high spatial and temporal resolution (Bogena et al., 2010; Bogena, Weuthen, et al., 2022). Each end device unit was equipped with eight SMT100 sensors (Truebner GmbH) (Bogena et al., 2017), which were installed within 5 m distance of each EGR monitoring station. Four of these sensors were installed at a depth of 5 cm, and the other four sensors were installed at a depth of 15 cm. The sensors at 5 cm were assumed to represent the SM of the top 10 cm of soil, and the sensors at 15 cm were assumed to represent the SM of the top 10–20 cm of soil. SM was measured with a temporal resolution of 15 min. Reference SM measurements during and 3 h after precipitation were not considered to obtain a dataset that is consistent with the EGR measurements filtered for the wash-out of radon progenies. Afterward, the mean SM time series measured at 5- and 15-cm depth were averaged to obtain a representative estimate of the moisture content for the top 20 cm of soil.

3.5 | Soil dry bulk density measurements

For the determination of the dry bulk density of soil at TS1 and TS2, we collected three soil cores within 5 m distance of each EGR monitoring station using a Humax soil auger. The length of each core was 30 cm, and the diameter was 5 cm. Each core was subdivided into six subsamples of 5 cm length, and the dry bulk density was estimated using the oven drying method (105°C for 48 h) for each subsample. The average dry bulk density of the top four samples of each core was used to calculate the mean dry bulk density of the top 20 cm of soil for both sites.

4 | RESULTS

4.1 | Environmental gamma radiation

The EGR measurements with 10-min resolution showed occasional spike-like patterns (Figure 4). As expected, these spikes were associated with precipitation events. After using the filter to remove EGR data during and 3 h after precipitation, the spikes were successfully removed. Similar results were obtained for both sites. This confirms that atmospheric radon progenies that have reached the ground by precipitation are responsible for the short-term transient increases in the EGR activity (Bottardi et al., 2020).

A significant (at $p < 0.05$) inverse relationship with a correlation coefficient ranging from −0.37 to −0.43 was observed between the daily average EGR and daily average atmospheric pressure for both test sites (Figure 5). Baciu et al. (2006) reported a medium to strong negative correlation (−0.57 to −0.21) between EGR and atmospheric pressure. As discussed previously, this is attributed to the effect of atmospheric pressure on the SCR, which contributes substantially to the EGR. In contrast, a significant positive relationship with a correlation coefficient ranging from 0.47 to 0.58 was found between the daily average EGR and daily average incoming neutron flux for both test sites (Figure 5). The correlation was stronger than that associated with the effect of atmospheric pressure. This is consistent with Dombrowski and Wissmann (2008), who reported that the relative variation of the EGR may range from −56% to 56% due to atmosphere pressure differences, while it could range from −30% to 100% for differences in incoming neutron flux.

Figure 6 shows the measured EGR for both test sites with hourly, daily, and weekly running averages after filtering for wash-out effects associated with precipitation. The average EGR of the two stations varied from ∼87 to 96 nSv h^{-1} during the study period (Table 1). The raw data with a 10-min temporal resolution were very noisy due to the uncertainty in the count rate and hence not shown in Figure 6. It is evident that temporal averaging reduced this noise strongly. For example, the standard deviation of the raw data for TS1 was 5.14 nSv h^{-1}, and it decreased to 2.13 nSv h^{-1} for the daily-averaged data and 1.84 nSv h^{-1} for the weekly averaged data. Hence, the uncertainty in EGR measurements decreased with the longer integration time, which agrees with the findings of Stöhlker et al. (2019).

4.2 | Terrestrial gamma radiation

The average weekly EGR was used to calculate the weekly TGR for both test sites (Figure 7) using Equations (16) and (18). The mean TGR of all sites varied from 44.71 to 54.28 nSv h^{-1} (Table 2). The standard deviation of the daily TGR (1.67 nSv h^{-1}) was found to be lower than the standard deviation of the daily EGR (1.84 nSv h^{-1}) for both sites (Tables 1 and 2). This suggests that some variation in the EGR associated with SCR was successfully removed. A second indication of the adequacy of the procedure to remove the SCR contribution from the EGR is that the correlation between extracted TGR and atmospheric pressure as well as incoming neutron flux was considerably lower than in the case of EGR (Table 3). For example, the correlation coefficient with atmospheric pressure was −0.43 for the EGR, while it was only 0.03 for the TGR (Table 3) in case of TS2. A third indication of the effectiveness of the correction procedure is that the correlation of the EGR between the two test sites decreased from 0.92 to 0.85 after removing the contribution of SCR from the EGR. The reason behind this decreased correlation of the TGR between the two sites is likely due to the increased

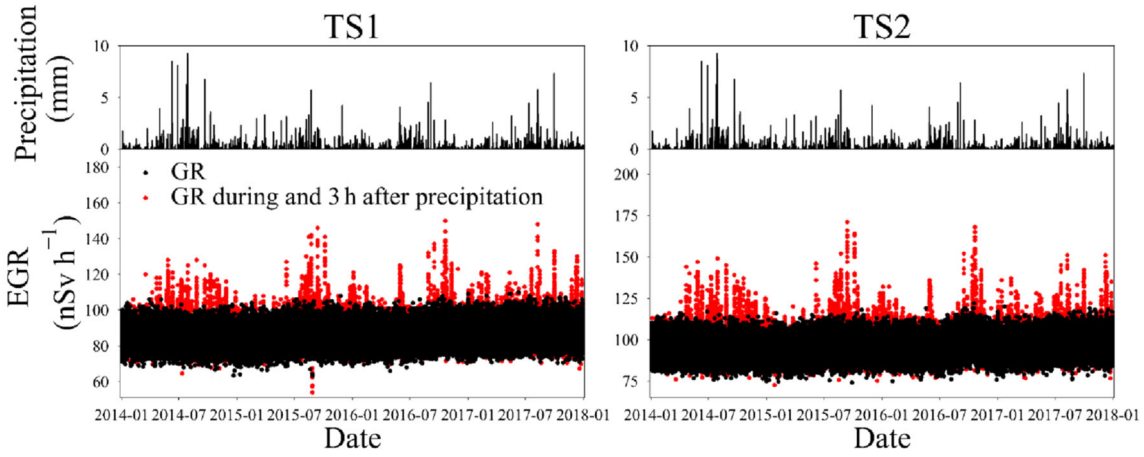

FIGURE 4 Influence of precipitation on the environmental gamma radiation (EGR) measurements for test site 1 (TS1) and test site 2 (TS2). The top plots show precipitation, and the bottom plots show EGR measurements. All the measurements are shown at 10-min resolution.

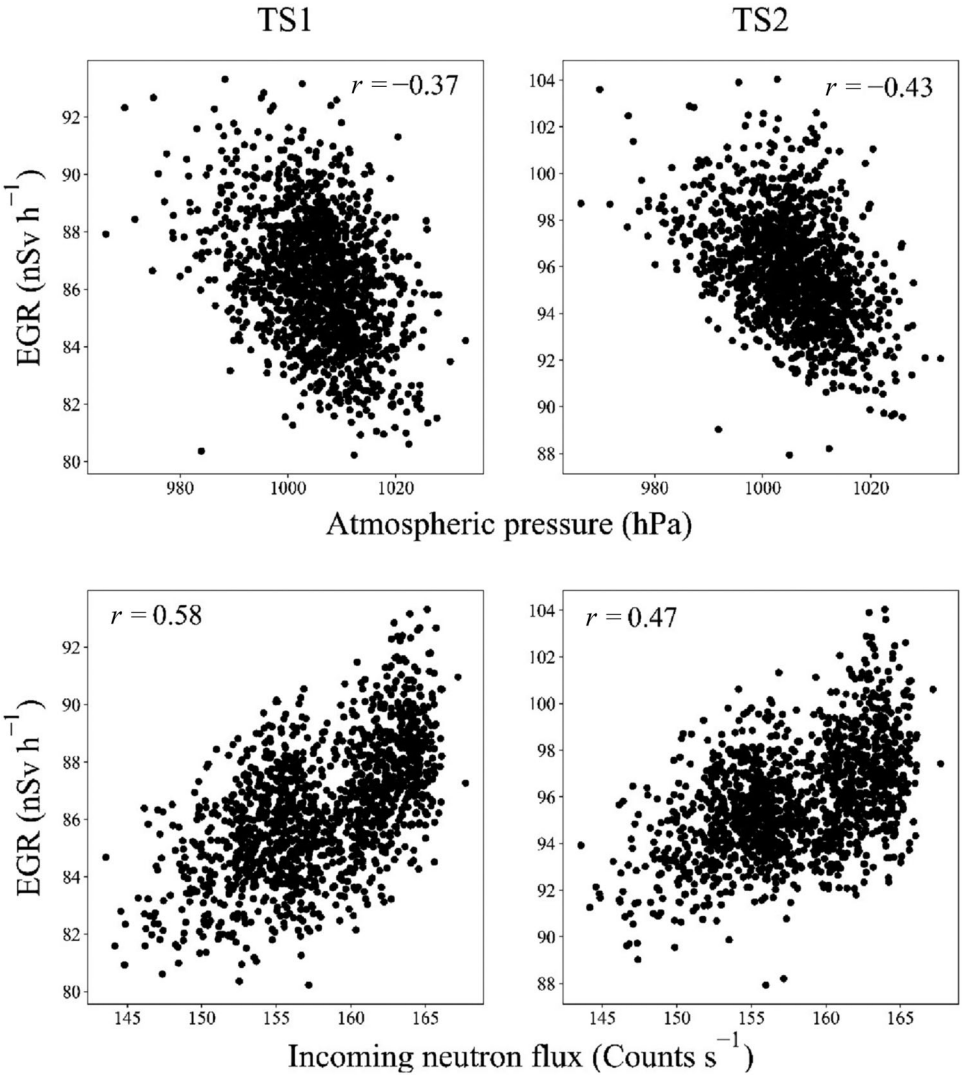

FIGURE 5 Correlation of the daily environmental gamma radiation (EGR) with atmospheric pressure and incoming neutron flux for test site 1 (TS1) and test site 2 (TS2).

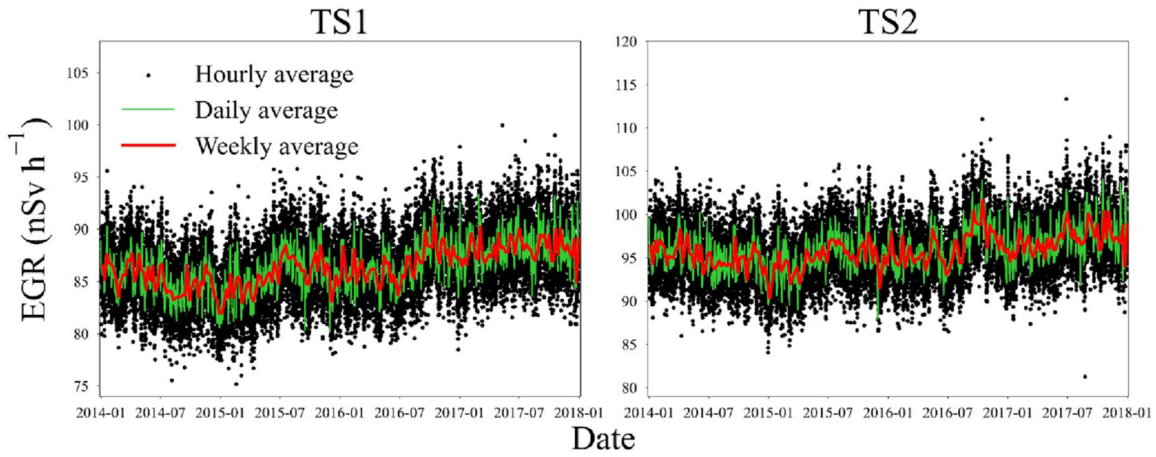

FIGURE 6 Filtered environmental gamma radiation (EGR) measurements for test site 1 (TS1) and test site 2 (TS2) for different integration times.

TABLE 1 General statistics of the environmental gamma radiation (EGR) for both test sites.

		Standard deviation (nSv h^{-1})			
Test site	**Mean (nSv h^{-1})**	**10-min data**	**Hourly average**	**Daily average**	**Weekly average**
1	86.35	5.14	2.94	2.13	1.84
2	95.84	5.39	3.10	2.31	1.84

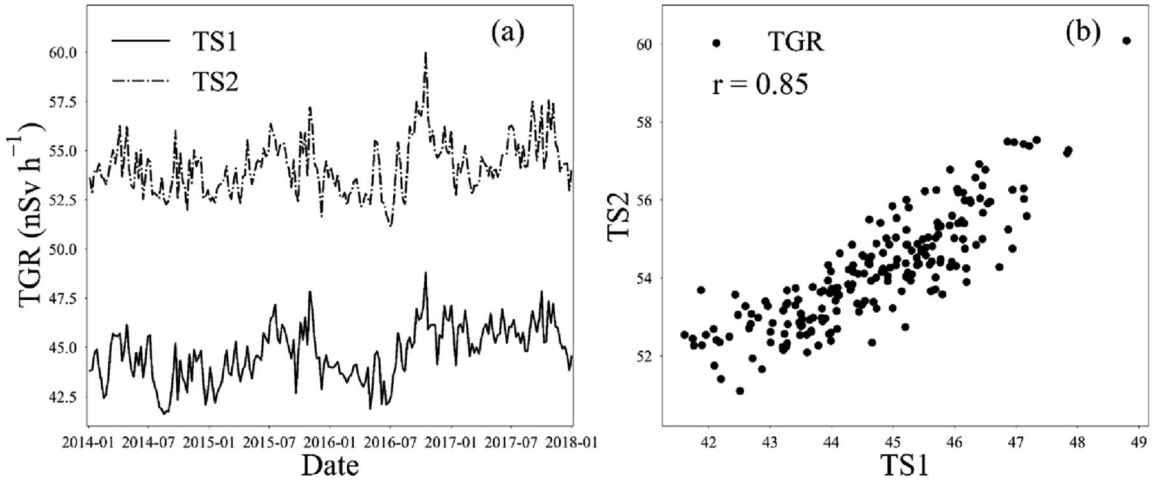

FIGURE 7 Weekly terrestrial gamma radiation (TGR) for test site 1 (TS1) and test site 2 (TS2) as well as the correlation between the TGR of both sites.

importance of site-specific variation related to SM after removing the SCR component.

4.3 | Estimating soil moisture from terrestrial gamma radiation

The weekly TGR was calibrated against the reference SM (top plots in Figure 8) for a period of 4 years to establish a functional relationship using Equation (14) for TS1. A shorter period was considered for TS2 because reference SM data were lost due to a technical problem. Analysis of the soil cores showed that the mean dry bulk density was 1.1 g cm^{-3} for TS1 and 1.0 g cm^{-3} for TS2. For the calibration, a weekly resolution was considered instead of daily resolution because the correlation between the TGR and reference SM was significantly higher with longer integration time for both sites. For example, the correlation coefficient was −0.59 between the

TABLE 2 Key statistics of the extracted weekly terrestrial gamma radiation (TGR) for both test sites.

Test site	Mean (nSv h^{-1})	Maximum (nSv h^{-1})	Minimum (nSv h^{-1})	Standard deviation (nSv h^{-1})
1	44.71	50.55	36.71	1.67
2	54.28	61.01	46.53	1.76

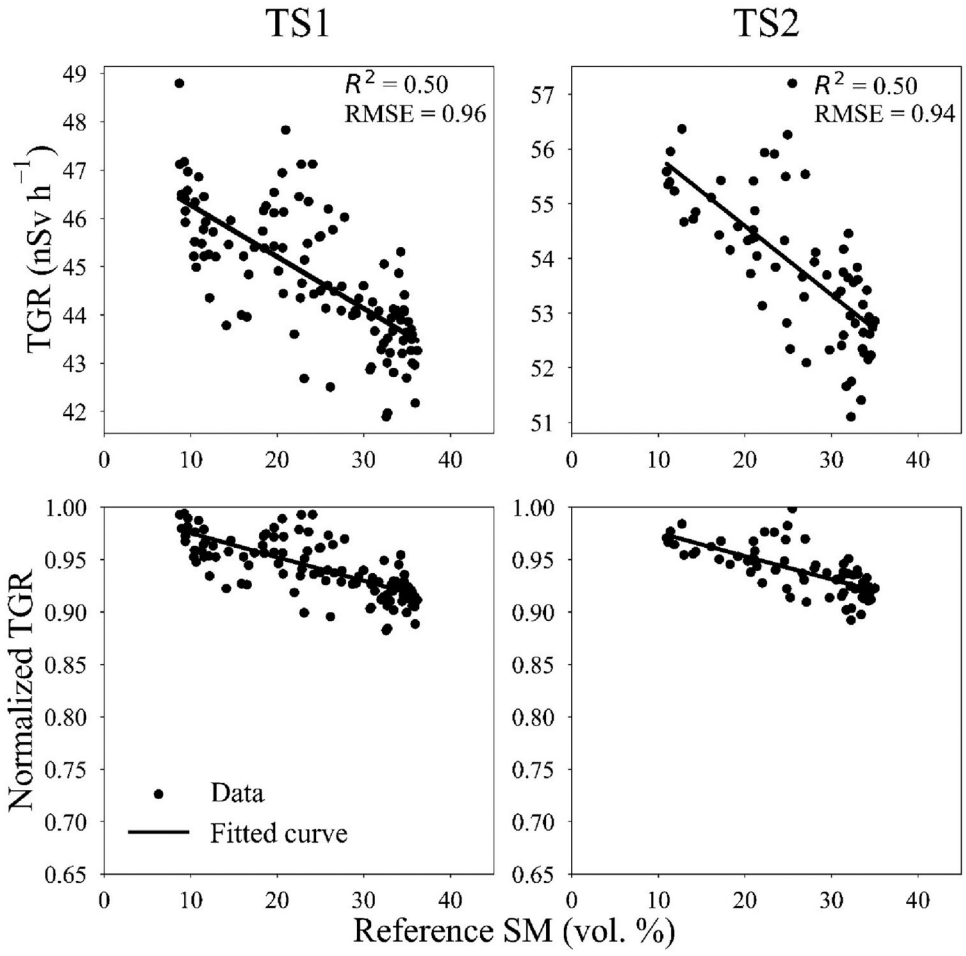

FIGURE 8 Weekly absolute (top) and normalized (bottom) terrestrial gamma radiation (TGR) as a function of weekly reference soil moisture (SM) for test site 1 (TS1) and test site 2 (TS2). R^2 indicates the coefficient of determination, and root mean square error (RMSE) is the root mean square error.

TABLE 3 Correlation of environmental gamma radiation (EGR) or terrestrial gamma radiation (TGR) with atmospheric pressure and incoming neutron flux.

Test site	Correlation coefficient (r)			
	Atmospheric pressure		Incoming neutron flux	
	EGR	TGR	EGR	TGR
1	−0.37	0.14	0.58	0.33
2	−0.43	0.03	0.47	0.20

TABLE 4 Results for the calibration parameters for both test sites using reference SoilNet soil moisture (SM) measurements obtained by averaging measurements at 5-cm and 15-cm depth.

Test site	$R_{TGR,dry}$	α
1	47.46	0.28
2	57.27	0.25

Note: $R_{TGR,dry}$—maximum terrestrial gamma radiation when the soil is completely dry; α—the effective ratio of TGR mass attenuation coefficients for water and solid phases.

daily TGR and reference SM, while it was −0.71 between the weekly TGR and reference SM for TS1. The calibrated parameters are provided in Table 4. The fitted values for $R_{TGR,dry}$ were 47.5 and 57.3 nSv h^{-1} for TS1 and TS2, respectively. These values were 3–4 nSv h^{-1} higher than the maximum

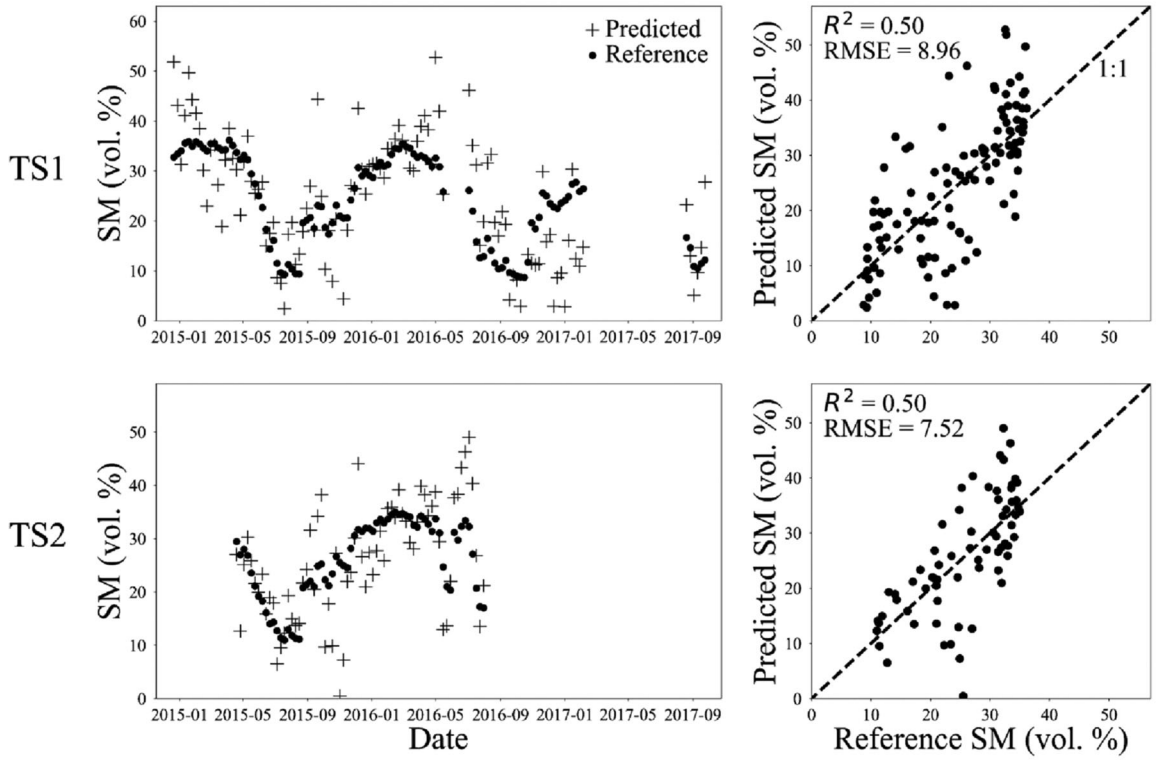

FIGURE 9 Seasonal dynamics (left) and reference versus predicted (right) soil moisture (SM) for test site 1 (TS1) and test site 2 (TS2). A shorter period was considered for TS2, as there was a data gap in the reference SM data due to a technical defect.

measured TGR for both test sites (Table 2) because the soils were not fully dry in the course of the field experiment. The observed differences in $R_{TGR,dry}$ are likely related to site-specific characteristics such as differences in radionuclide concentrations of soil-forming minerals (Stöhlker et al., 2012) or shielding effects, for example, shielding due to the presence of a concrete road or building within the measurement footprint (Dombrowski et al., 2017).

We found that the theoretical α value of 1.11, which only considers the contribution of high-energy radionuclides (0.4–1.46 MeV) for TGR, did not describe the observed relationship well. Instead, the calibrated value for α was around 0.3 for both test sites. This relatively low value suggests a strong contribution of low-energy TGR with an energy range below 0.10 MeV (Figure S1). Consequently, the magnitude of the decrease in TGR with an increase in SM was lower for the present study (bottom plots in Figure 8) than in the case of spectrometric measurements in the high-energy range for which $\alpha = 1.11$ applies (Figure 2). Despite the differences in $R_{TGR,dry}$ between the two test sites (Table 4), the almost identical calibrated α value indicates that the energy spectrum was similar for both sites. This provides confidence in the robustness of the developed calibration models for the current study and suggests that the methodology developed in this study can be extended to other sites for estimating SM from EGR.

After calibration, SM was predicted from the TGR and compared with reference SM measurements (Figure 9). The seasonal variation of SM was reasonably well captured by the TGR. A comparison of predicted and reference SM provided an $R^2 = 0.50$ and an root mean square error (RMSE) of 7–9 vol.%. This RMSE is relatively high when compared to other in situ SM measurements. For example, Cui et al. (2020) and Y. Lu et al. (2017) predicted SM using ground penetrating radar (GPR) with an average RMSE ranging from 0.3 to 8 vol.% for a wide variety of soil types. Moreover, Akbar et al. (2005) reported an RMSE ranging from 2 to 5 vol.% while estimating SM using electromagnetic induction. However, the obtained RMSE is similar to that of satellite-based SM estimates. For example, Liu et al. (2022) estimated the SM of the top 5 cm soil with an RMSE of 7 vol.% using satellite data.

5 | DISCUSSION

We found a strong negative relationship between SM and TGR ($r = -0.59$ and -0.71 for the daily and weekly measurements, respectively) for a multi-year period using commercial proportional counter-tube EGR sensors similar to the ones typically used in the EURDEP network. This is consistent with the results presented by Stöhlker et al. (2012), who

investigated the correlation between SM and TGR for a period of 2 months at seven different experimental sites, also using EGR sensors similar to the type of sensors used in the EUR-DEP network. They obtained correlation coefficients between daily TGR and SM content ranging from −0.59 to −0.84. In contrast, Gianessi, Polo, Stevanato, Lunardon, Francke et al. (2022) reported a weaker correlation between SM and TGR for a period of 3 months in an Italian agricultural field. In that study, EGR was determined using a novel scintillator-based sensor developed to jointly estimate TGR, cosmic neutrons, and cosmic muons flux. These reported variations in correlation strength may be due to differences in site characteristics, for example, soil properties, or differences in the detection characteristics of the EGR sensors.

For the current study, the EGR-based SM estimates varied with a greater amplitude compared to the reference SM estimates and consequently resulted in relatively high prediction errors. This higher prediction error may have several reasons, which are discussed in more detail below. First of all, the low value for the calibrated parameter α for both sites indicates that a considerable fraction of the EGR measured with the sensors used for the current study has a low energy. Hence, those sensors might not fully capture the TGR signals originating from the decay of typical terrestrial radioisotopes such as ^{40}K, ^{232}Th, and ^{238}U at high energy, which have been shown to provide a distinct response to SM change. In addition, low-energy EGR is associated with more noise compared to high-energy EGR, leading to a high error for SM estimation from the terrestrial component of EGR. In a future study, nuclide-specific spectral gamma radiation measurements should be acquired in addition to EGR measurements. A joint interpretation may help to better understand the sources of inaccuracy for estimating SM from TGR obtained with proportional counters.

The low energy of the observed EGR also has implications for the measurement footprint. In the case of high-energy radionuclides, such as ^{40}K (1.46 MeV), the horizontal footprint is approximately 15 m and the vertical footprint is approximately 30 cm (Baldoncini et al., 2018). The measurement footprint is smaller for low-energy gamma radiation (see Figure S4). For example, the vertical footprint is reduced to ∼5 cm at 0.04 MeV. This reduced measurement footprint may be responsible for the higher prediction error. The reference SM sensors installed at 5-cm depth, representative of top 10 cm soil, might not be fully representative of the SM dynamics near the soil surface (0–5 cm). Thus, the use of more dense vertical reference SM measurements, specifically for the top 10 cm soil, may improve the SM prediction accuracy. Since soil is both the source and the attenuating material, it is obvious that gamma radiation originating in the upper layer of soil needs to travel a shorter distance to reach the EGR sensors. Therefore, reference SM measurements weighted according to the depth sensitivity should also be considered in future studies, especially when the SM distribution is heterogeneous within the soil profile.

Another possible explanation for the higher prediction error is the unaccounted effect of water present in aboveground biomass within the measurement footprint of EGR sensors. As the sensors were located at about 1 m height above the ground, mainly tree stems and undergrowth could attenuate the TGR signal rather than the tree canopy. To test this possibility, we roughly subdivided the measurements into two periods: the growing season (April to September) and the nongrowing season (October to March), when deciduous trees shed leaves due to unfavorable weather conditions. A clustering of datapoints was observed when this subdivision was applied to the data shown in Figure 8 (see Figure S5). Most of the observations during the growing period fall below the fitted model, possibly suggesting that the TGR signals were further attenuated by the water content present in aboveground biomass. In contrast, EGR was typically higher for most of the observations during the nongrowing season due to the lack of this additional attenuation by above-ground biomass. Because of this biomass effect, SM was overestimated during the growing season and underestimated outside of this period (see Figure S6). Baldoncini et al. (2019) developed a biomass correction method for TGR signals related to the high-energy radioisotope ^{40}K, but more work is required to extend this approach to the EGR measurements considered in this study. This should be explored in a follow-up study where accurate information on biomass development is available.

Finally, the prediction accuracy may have been affected by other factors such as variability in soil and atmospheric radon concentrations, the soil-skyshine contribution, and uncertainties in the contribution of SCR. It is well known that soil and atmospheric radon concentrations show complex short-term and long-term variability, which might affect TGR measurements (Siino et al., 2019). The short-term variability (e.g., daily cycles, multi-day cycles) in soil radon concentration occurs due to the site-dependent variability in climatic variables such as temperature and atmospheric pressure, while the long-term variability (e.g., annual cycle) is also related to the seasonal rainfall cycles along with the two above-mentioned variables (Siino et al., 2019). For the current study, the short-term variability in soil radon concentration is not relevant because we aggregated the data to a weekly timescale. However, the long-term variability in soil radon concentration may have influenced the measurements of the current study. After escaping from the soil, radon can migrate away from the point source as a result of the complex interplay between atmospheric and geological properties (van der Veeke et al., 2020). Stöhlker et al. (2019) reported that the airborne EGR originating from the atmospheric radon progenies can also cause considerable variability in TGR over a longer period.

Soil-skyshine represents the backscattering of TGR toward the earth surface by aboveground air from distant soil well

outside the measurement footprint (Sandness et al., 2009). Soil-skyshine was found to be a significant contributor to the natural background at low energies (<500 keV) and can even contribute up to 50% of the total background at 100 keV (Mitchell et al., 2009). As the EGR sensors used for the current study mostly measured low-energy EGR, it is possible that soil-skyshine contribution affected the EGR measurements resulting in a lower SM prediction accuracy.

For the current study, the variability in SCR was calculated assuming a strong relationship between cosmic neutron and muon flux, and corrections were made using incoming neutron monitoring data only. However, Gianessi, Polo, Stevanato, Lunardon, Francke et al. (2022) noted substantial differences between neutron flux measurements from the neutron monitor database and a locally measured muon flux. This deviation in muon flux can be incurred due to the changes of atmospheric temperature leading to seasonal variation in muon flux (Wissmann et al., 2005). Hence, the procedure to eliminate the contribution of SCR may need to be improved using local measurements. This could be achieved using collocated cosmic-ray neutron or muon sensors.

6 | CONCLUSIONS

In this study, we investigated the potential of EGR measurements to determine SM for two sites located in Germany. For this, we filtered the EGR measurements to eliminate the contribution of atmospheric radon wash-out. After this, we separated the terrestrial component of EGR by removing the contribution of SCR. We installed reference in situ SM sensors within the measurement footprint of the EGR sensors to establish a relationship between EGR and SM and to evaluate the accuracy of EGR-based SM estimates. Based on our findings, we conclude that the terrestrial component of EGR used in this study provided weekly SM estimates with a relatively high error (7–9 vol.%), but the seasonal changes of SM were well reproduced. The possible sources of uncertainty that affected the accuracy of SM estimates include the importance of low-energy radiation in the measured EGR signals (including a skyshine contribution), additional attenuation by biomass water content, variability in soil and atmospheric radon concentration, and unavailability of local SCR measurements. These sources of uncertainty were found to be similar for both sites and should be investigated in more detail in future studies.

This study is a first step to estimate SM using the type of EGR measurements available in the EURDEP network. More investigations are needed to improve the SM prediction accuracy. Despite the low accuracy of the EGR-based SM estimates compared to other in situ measurements, we believe that this technique can compete with satellite-based remote sensing techniques to estimate root-zone SM on the European continental scale because of its deeper penetration depth and long data record.

AUTHOR CONTRIBUTIONS

Sonia Akter: Data curation; formal analysis; investigation; methodology; validation; visualization; writing—original draft. **Johan Alexander Huisman**: Conceptualization; data curation; formal analysis; funding acquisition; investigation; methodology; project administration; resources; supervision; validation; writing—review and editing. **Heye Reemt Bogena**: Conceptualization; data curation; funding acquisition; investigation; methodology; resources; supervision; validation; writing—review and editing.

ACKNOWLEDGMENTS

We thank Bernd Schilling, Ansgar Weuthen, and Ralf Eckert for the technical support. We also thank Jie Mao for his contribution in the initial phase of this work. The position of Sonia Akter was funded by the Deutsche Forschungsgemeinschaft (DFG, German Research Foundation) – SFB 1502/1–2022 - Projektnummer: 450058266. We also received support from TERENO (TERrestrial Environmental Observatories) funded by the Helmholtz-Gemeinschaft. We are thankful to the Umgebungsüberwachung S-U (Environmental Monitoring) department of Sicherheit und Strahlenschutz (Safety and Radiation Protection) division in Forschungszentrum Jülich for providing us with the gamma radiation data. We also acknowledge the real-time neutron monitoring database (NMDB) funded by EU-FP7.

CONFLICT OF INTEREST STATEMENT

The authors declare no conflicts of interest.

DATA AVAILABILITY STATEMENT

The complete data set employed in this study has been made publicly available on the DETECT-Geonetwork platform (https://detect-z03.geoinformation.net/geonetwork/srv/eng/catalog.search#/search). Furthermore, climate data used in this study is available on the TERENO (Terrestrial Environmental Observatories) data portal (https://ddp.tereno.net/ddp/).

ORCID

Sonia Akter https://orcid.org/0000-0003-1706-3940
Johan Alexander Huisman https://orcid.org/0000-0002-1327-0945
Heye Reemt Bogena https://orcid.org/0000-0001-9974-6686

REFERENCES

Akbar, M. A., Kenimer, A. L., Searcy, S. W., & Torbert, H. A. (2005). Soil water estimation using electromagnetic induction. *Transactions of the ASAE*, *48*, 129–135. https://doi.org/10.13031/2013.17955

Andreasen, M., Jensen, K. H., Bogena, H., Desilets, D., Zreda, M., & Looms, M. C. (2020). Cosmic ray neutron soil moisture estimation using physically based site-specific conversion functions. *Water Resources Research*, *56*(11), e2019WR026588. https://doi.org/10.1029/2019wr026588

Baciu, A. C., Baciu, A. C., & Baciu, A. C. (2006). Outdoor absorbed dose rate in air in relation to airborne natural radioactivity and meteorological conditions at Bucharest (Romania). *Journal of Radioanalytical and Nuclear Chemistry*, *268*, 3–14. https://doi.org/10.1007/s10967-006-0116-7

Baldoncini, M., Albéri, M., Bottardi, C., Chiarelli, E., Raptis, K. G., Strati, V., & Mantovani, F. (2018). Investigating the potentialities of Monte Carlo simulation for assessing soil water content via proximal gamma-ray spectroscopy. *Journal of Environmental Radioactivity*, *192*, 105–116. https://doi.org/10.1016/j.jenvrad.2018.06.001

Baldoncini, M., Albéri, M., Bottardi, C., Chiarelli, E., Raptis, K. G., Strati, V., & Mantovani, F. (2019). Biomass water content effect on soil moisture assessment via proximal gamma-ray spectroscopy. *Geoderma*, *335*, 69–77. https://doi.org/10.1016/j.geoderma.2018.08.012

Beamish, D. (2013). Gamma ray attenuation in the soils of Northern Ireland, with special reference to peat. *Journal of Environmental Radioactivity*, *115*, 13–27. https://doi.org/10.1016/j.jenvrad.2012.05.031

Binley, A., Hubbard, S. S., Huisman, J. A., Revil, A., Robinson, D. A., Singha, K., & Slater, L. D. (2015). The emergence of hydrogeophysics for improved understanding of subsurface processes over multiple scales. *Water Resources Research*, *51*, 3837–3866. https://doi.org/10.1002/2015wr017016

Bleher, M., Doll, H., Harms, W., & Stöhlker, U. (2014). INTERCAL: Long-term inter-comparison experiment for dose rate and spectrometric probes. *Radiation Protection Dosimetry*, *160*(4), 306–310.

Bobik, P., Kudela, K., Pastircak, B., Santangelo, A., Bertaina, M., Shinozaki, K., Fenu, F., Szabelski, J., & Urbar, J. (2012). Distribution of secondary particles intensities over Earth's surface: Effect of the geomagnetic field. *Advances in Space Research*, *50*, 986–996. https://doi.org/10.1016/j.asr.2012.06.010

Bogena, H. R., Herbst, M., Huisman, J. A., Rosenbaum, U., Weuthen, A., & Vereecken, H. (2010). Potential of wireless sensor networks for measuring soil water content variability. *Vadose Zone Journal*, *9*, 1002–1013. https://doi.org/10.2136/vzj2009.0173

Bogena, H. R., Huisman, J. A., Güntner, A., Hübner, C., Kusche, J., Jonard, F., Vey, S., & Vereecken, H. (2015). Emerging methods for noninvasive sensing of soil moisture dynamics from field to catchment scale: A review. *WIREs Water*, *2*, 635–647. https://doi.org/10.1002/wat2.1097

Bogena, H. R., Huisman, J. A., Schilling, B., Weuthen, A., & Vereecken, A. (2017). Effective calibration of low-cost soil water content sensors. *Sensors*, *17*, 208. https://doi.org/10.3390/s17010208

Bogena, H. R., Schrön, M., Jakobi, J., Ney, P., Zacharias, S., Andreasen, M., Baatz, R., Boorman, D., Berk Duygu, M., Eguibar-Galán, M. A., Fersch, B., Franke, T., Geris, J., González Sanchis, M., Kerr, Y., Korf, T., Mengistu, Z., Mialon, A., Nasta, P., … Vereecken, H. (2022). COSMOS-Europe: A European network of cosmic-ray neutron soil moisture sensors. *Earth System Science Data*, *14*, 1125–1151. https://doi.org/10.5194/essd-14-1125-2022

Bogena, H. R., Weuthen, A., & Huisman, J. A. (2022). Recent developments in wireless soil moisture sensing to support scientific research and agricultural management. *Sensors*, *22*, 9792. https://doi.org/10.3390/s22249792

Bossew, P., Cinelli, G., Hernández-Ceballos, M., Cernohlawek, N., Gruber, V., Dehandschutter, B., Menneson, F., Bleher, M., Stöhlker, U., Hellmann, I., Weiler, F., Tollefsen, T., Tognoli, P. V., & de Cort, M. (2017). Estimating the terrestrial gamma dose rate by decomposition of the ambient dose equivalent rate. *Journal of environmental radioactivity*, *166*, 296–308. https://doi.org/10.1016/j.jenvrad.2016.02.013

Bottardi, C., Albéri, M., Baldoncini, M., Chiarelli, E., Montuschi, M., Raptis, K. G. C., Serafini, A., Strati, V., & Mantovani, F. (2020). Rain rate and radon daughters' activity. *Atmospheric Environment*, *238*, 117728. https://doi.org/10.1016/j.atmosenv.2020.117728

Carroll, T. R. (1981). Airborne soil moisture measurement using natural terrestrial gamma radiation. *Soil Science*, *132*, 358–366. https://doi.org/10.1097/00010694-198111000-00006

Cui, F., Ni, J., Du, Y., Zhao, Y., & Zhou, Y. (2020). Soil water content estimation using ground penetrating radar data via group intelligence optimization algorithms: An application in the Northern Shaanxi coal mining area. *Energy Exploration & Exploitation*, *39*, 318–335. https://doi.org/10.1177/0144598720973369

Dombrowski, H., Bleher, M., Cort, M. D., Dabrowski, R., Neumaier, S., & Stöohlker, U. (2017). Recommendations to harmonize European early warning dosimetry network systems. *Journal of Instrumentation*, *12*, P12024–P12024. https://doi.org/10.1088/1748-0221/12/12/p12024

Dombrowski, H., & Wissmann, F. (2008). Meteorological influences on the results of area dose rate measurements. *Kerntechnik*, *73*, 113–117. https://doi.org/10.3139/124.100554

Ghajarnia, N., Kalantari, Z., Orth, R., & Destouni, G. (2020). Close co-variation between soil moisture and runoff emerging from multi-catchment data across Europe. *Scientific Reports*, *10*, Article 4817. https://doi.org/10.1038/s41598-020-61621-y

Gianessi, S., Polo, M., Stevanato, L., Lunardon, M., & Baroni, G. (2022). Comparison of cosmic-ray neutron sensing and gamma-ray spectrometry for non-invasive soil moisture estimation over a large cropped field. In *2022 IEEE workshop on metrology for agriculture and forestry (MetroAgriFor)* (pp. 48–52). IEEE. https://doi.org/10.1109/metroagrifor55389.2022.9964647

Gianessi, S., Polo, M., Stevanato, L., Lunardon, M., Francke, T., Oswald, S., Ahmed, H., Tolosa, A., Weltin, G., Dercon, G., Fulajtar, E., Heng, L., & Baroni, G. (2022). Testing a novel sensor design to jointly measure cosmic-ray neutrons, muons and gamma rays for non-invasive soil moisture estimation. *Geoscientific Instrumentation, Methods and Data Systems*, *13*(1), 9–25. https://doi.org/10.5194/gi-2022-20

Grasty, R. L. (1976). Applications of gamma radiation in remote sensing. In E. Schanda (Ed.), *Remote sensing for environmental sciences* (pp. 257–276). Ecological studies. Springer. https://doi.org/10.1007/978-3-642-66236-2_7

Grasty, R. L. (1987). *The design, construction, and application of airborne gamma-ray spectrometer calibration pads – Thailand*. Geological Survey of Canada.

Grasty, R. L. (1997). Radon emanation and soil moisture effects on airborne gamma-ray measurements. *Geophysics*, *62*, 1379–1385. https://doi.org/10.1190/1.1444242

Greenfield, M. B., Domondon, A. T., Okamoto, N., & Watanabe, I. (2002). Variation in γ-ray count rates as a monitor of precipitation rates, radon concentrations, and tectonic activity. *Journal of Applied Physics*, *91*, 1628–1633. https://doi.org/10.1063/1.1426248

IAEA. (2003). *Guidelines for radioelement mapping using gamma rayspectrometry data*. https://www-pub.iaea.org/MTCD/Publications/PDF/te_1363_web.pdf

Kessler, P., Behnke, B., Dabrowski, R., Dombrowski, H., Röttger, A., & Neumaier, S. (2018). Novel spectrometers for environmental dose rate monitoring. *Journal of Environmental Radioactivity*, *187*, 115–121. https://doi.org/10.1016/j.jenvrad.2018.01.020

Liu, Q., Gu, X., Chen, X., Mumtaz, F., Liu, Y., Wang, C., Yu, T., Zhang, Y., Wang, D., & Zhan, Y. (2022). Soil moisture content retrieval from remote sensing data by artificial neural network based on sample optimization. *Sensors*, *22*, 1611. https://doi.org/10.3390/s22041611

Loijens, H. S. (1980). Determination of soil water content from terrestrial gamma radiation measurements. *Water Resources Research*, *16*, 565–573. https://doi.org/10.1029/wr016i003p00565

Løvborg, L. (1984). *The calibration of portable and airborne gamma-ray spectrometers—Theory, problems, and facilities*. Technical University of Denmark, Risø National laboratory.

Lu, N. (2019). Linking soil water adsorption to geotechnical engineering properties. In N. Lu & J. K. Mitchell (Eds.), *Geotechnical fundamentals for addressing new world challenges* (pp. 93–139). Springer International Publishing. https://doi.org/10.1007/978-3-030-06249-1_4

Lu, Y., Song, W., Lu, J., Wang, X., & Tan, Y. (2017). An examination of soil moisture estimation using ground penetrating radar in Desert Steppe. *Water*, *9*, 521. https://doi.org/10.3390/w9070521

Minty, B. R. (1997). Fundamentals of airborne gamma-ray spectrometry. *Journal of Australian Geology and Geophysics*, *17*, 39–50.

Mishra, A., Vu, T., Veettil, A. V., & Entekhabi, D. (2017). Drought monitoring with soil moisture active passive (SMAP) measurements. *Journal of Hydrology*, *552*, 620–632. https://doi.org/10.1016/j.jhydrol.2017.07.033

Mitchell, A. L., Borgardt, J. D., & Kouzes, R. T. (2009). *Skyshine contribution to gamma ray background between 0 and 4 MeV* (PNNL-18666). U.S. Department of Energy. https://doi.org/10.2172/990599

Moragoda, N., Kumar, M., & Cohen, S. (2022). Representing the role of soil moisture on erosion resistance in sediment models: Challenges and opportunities. *Earth-Science Reviews*, *229*, 104032. https://doi.org/10.1016/j.earscirev.2022.104032

Morison, I. (2008). *Introduction to astronomy and cosmology*. John Wiley & Sons.

Neumaier, S., & Dombrowski, H. (2014). EURADOS intercomparisons and the harmonisation of environmental radiation monitoring. *Radiation Protection Dosimetry*, *160*(4), 297–305. https://doi.org/10.1093/rpd/ncu002

NIST. (2024). *X-ray mass attenuation coefficients*. https://physics.nist.gov/PhysRefData/XrayMassCoef/tab4.html

Peck, E. L., Bissell, V. C., Jones, E. B., & Burge, D. L. (1971). Evaluation of snow water equivalent by airborne measurement of passive terrestrial gamma radiation. *Water Resources Research*, *7*, 1151–1159. https://doi.org/10.1029/wr007i005p01151

Pignotti, G., Crawford, M., Han, E., Williams, M. R., & Chaubey, I. (2023). SMAP soil moisture data assimilation impacts on water quality and crop yield predictions in watershed modeling. *Journal of Hydrology*, *617*, 129122. https://doi.org/10.1016/j.jhydrol.2023.129122

Ran, Q., Wang, J., Chen, X., Liu, L., Li, J., & Ye, S. (2022). The relative importance of antecedent soil moisture and precipitation in flood generation in the middle and lower Yangtze River basin. *Hydrology and Earth System Sciences*, *26*, 4919–4931. https://doi.org/10.5194/hess-26-4919-2022

REMon. (2023). *EURDEP advanced map*. European Commission Joint Research Center. https://remap.jrc.ec.europa.eu/Advanced.aspx

REMon. (2024a). *EURDEP*. European Commission Joint Research Center. https://remon.jrc.ec.europa.eu/About/Rad-Data-Exchange

REMon. (2024b). *EURDEP atlas of natural radiation*. European Commission Joint Research Center. https://remap.jrc.ec.europa.eu/Atlas.aspx

Rosolem, R., Shuttleworth, W. J., Zreda, M., Franz, T. E., Zeng, X., & Kurc, S. A. (2013). The effect of atmospheric water vapor on neutron count in the cosmic-ray soil moisture observing system. *Journal of Hydrometeorology*, *14*(5), 1659–1671. https://doi.org/10.1175/JHM-D-12-0120.1

Sandness, G. A., Schweppe, J. E., Hensley, W. K., Borgardt, J. D., & Mitchell, A. L. (2009). Accurate modeling of the terrestrial gamma-ray background for homeland security applications. In *2009 IEEE nuclear science symposium conference record (NSS/MIC)* (pp. 126–133). IEEE. https://doi.org/10.1109/nssmic.2009.5401843

Sangiorgi, M., Hernández-Ceballos, M. A., Jackson, K., Cinelli, G., Bogucarskis, K., De Felice, L., Patrascu, A., & De Cort, M. (2020). The European Radiological Data Exchange Platform (EURDEP): 25 years of monitoring data exchange. *Earth System Science Data*, *12*, 109–118. https://doi.org/10.5194/essd-12-109-2020

Siino, M., Scudero, S., Cannelli, V., Piersanti, A., & D'Alessandro, A. (2019). Multiple seasonality in soil radon time series. *Scientific Reports*, *9*(1), Article 8610. https://doi.org/10.1038/s41598-019-44875-z

Singh, N. K., Emanuel, R. E., McGlynn, B. L., & Miniat, C. F. (2021). Soil moisture responses to rainfall: Implications for runoff generation. *Water Resources Research*, *57*(9), e2020WR028827. https://doi.org/10.1029/2020wr028827

Stahlmann-Brown, P., & Walsh, P. (2022). Soil moisture and expectations regarding future climate: Evidence from panel data. *Climatic Change*, *171*(1–2), Article 1. https://doi.org/10.1007/s10584-022-03317-y

Stevanato, L., Baroni, G., Oswald, S. E., Lunardon, M., Mares, V., Marinello, F., Moretto, S., Polo, M., Sartori, P., Schattan, P., & Ruehm, W. (2022). An alternative incoming correction for cosmic-ray neutron sensing observations using local muon measurement. *Geophysical Research Letters*, *49*(6), e2021GL095383. https://doi.org/10.1029/2021gl095383

Stöhlker, U., Bleher, M., Conen, F., & Baenninger, D. (2012). Harmonization of ambient dose rate monitoring provides for large scale estimates of radon flux density and soil moisture changes. In *Sources and measurements of radon and radon progeny applied to climate and air quality studies* (pp. 53–64). International Atomic Energy Agency.

Stöhlker, U., Bleher, M., Doll, H., Dombrowski, H., Harms, W., Hellmann, I., Luff, R., Prommer, B., Seifert, S., & Weiler, F. (2019). The German dose rate monitoring network and implemented data harmonization techniques. *Radiation Protection Dosimetry*, *183*, 405–417. https://doi.org/10.1093/rpd/ncy154

Stöhlker, U., Bleher, M., Szegvary, T., & Conen, F. (2009). Intercalibration of gamma dose rate detectors on the European scale. *Radioprotection*, *44*, 777–784. https://doi.org/10.1051/radiopro/20095140

Strati, V., Albéri, M., Anconelli, S., Baldoncini, M., Bittelli, M., Bottardi, C., Chiarelli, E., Fabbri, B., Guidi, V., Raptis, K. G. C., Solimando, D., Tomei, F., Villani, G., & Mantovani, F. (2018). Modelling soil

water content in a tomato field: Proximal gamma ray spectroscopy and soil–crop system models. *Agriculture*, *8*, 60. https://doi.org/10.3390/agriculture8040060

Szegvary, T., Conen, F., Stöhlker, U., Dubois, G., Bossew, P., & de Vries, G. (2007). Mapping terrestrial-dose rate in Europe based on routine monitoring data. *Radiation Measurements*, *42*, 1561–1572. https://doi.org/10.1016/j.radmeas.2007.09.002

Terry, N., Day-Lewis, F. D., Lane, J. W., Johnson, C. D., & Werkema, D. (2023). Field evaluation of semi-automated moisture estimation from geophysics using machine learning. *Vadose Zone Journal*, *22*(2), e20246. https://doi.org/10.1002/vzj2.20246

Thermo. (2015). *Wide-range detector FHZ 621 G-L*. https://www.perlamar.ie/wp-content/uploads/pdf/thermo/FIXED_GAMMA_PROBES/FHZ_621%20G-L.pdf

Thompson, I. M. G., Bøtter-Jensen, L., Deme, S., Pernicka, F., & Sa´ez-Vergara, J. C. (1999). *Technical recommendations on measurements of external environmental gamma radiation doses. A report of EURADOS Working Group 12, 'Environmental Radiation Monitoring'* (Radiation Protection Report 106). Commission of the European Communities.

UNSCEAR. (2000). *Sources and effects of ionizing radiation* (UNSCEAR 2000 Report to the General Assembly, Vol. I). United Nations.

Vana, N., Hajek, M., & Berger, T. (2003). *Ambient dose equivalent H*(d)-an appropriate philosophy for radiation monitoring onboard aircraft and in space?* IRPA Regional Congress on Radiation Protection in Central Europe, Bratislava, Slovakia.

van der Veeke, S., Koomans, R., & Limburg, H. (2020). Using a gamma-ray spectrometer for soil moisture monitoring: Development of the gamma soil moisture sensor (gSMS). In *2020 IEEE international workshop on metrology for agriculture and forestry (MetroAgriFor)* (pp. 185–190). IEEE. https://doi.org/10.1109/metroagrifor50201.2020.9277560

Vereecken, H., Amelung, W., Bauke, S. L., Bogena, H., Brüggemann, N., Montzka, C., Vanderborght, J., Bechtold, M., Blöschl, G., Carminati, A., Javaux, M., Konings, A. G., Kusche, J., Neuweiler, I., Or, D., Steele-Dunne, S., Verhoef, A., Young, M., & Zhang, Y. (2022). Soil hydrology in the Earth system. *Nature Reviews Earth & Environment*, *3*, 573–587. https://doi.org/10.1038/s43017-022-00324-6

Wissmann, F. (2006). Variations observed in environmental radiation at ground level. *Radiation Protection Dosimetry*, *118*, 3–10. https://doi.org/10.1093/rpd/nci317

Wissmann, F., Dangendorf, V., & Schrewe, U. (2005). Radiation exposure at ground level by secondary cosmic radiation. *Radiation Measurements*, *39*, 95–104. https://doi.org/10.1016/j.radmeas.2004.03.025

Wissmann, F., Rupp, A., & Stöhlker, U. (2007). Characterization of dose rate instruments for environmental radiation monitoring. *Kerntechnik*, *72*, 193–198. https://doi.org/10.3139/124.100341

Wissmann, F., & Sáez-Vergara, J. C. (2006). Dosimetry of environmental radiation—A report on the achievements of EURADOS WG3. *Radiation Protection Dosimetry*, *118*, 167–175. https://doi.org/10.1093/rpd/ncl015

Yoshioka, K. (1989). Soil moisture gauge using terrestrial gamma-rays. *Nuclear Geophysics*, *3*, 397–401.

Zreda, M., Shuttleworth, W. J., Zeng, X., Zweck, C., Desilets, D., Franz, T., & Rosolem, R. (2012). COSMOS: The COsmic-ray Soil Moisture Observing System. *Hydrology and Earth System Sciences*, *16*, 4079–4099. https://doi.org/10.5194/hess-16-4079-2012

SUPPORTING INFORMATION

Additional supporting information can be found online in the Supporting Information section at the end of this article.

How to cite this article: Akter, S., Huisman, J. A., & Bogena, H. R. (2024). Estimating soil moisture from environmental gamma radiation monitoring data. *Vadose Zone Journal*, *23*, e20384. https://doi.org/10.1002/vzj2.20384